

Clinical and Experimental Hypertension



ISSN: (Print) (Online) Journal homepage: https://www.tandfonline.com/loi/iceh20

Establishment of a canine model of pulmonary arterial hypertension induced by dehydromonocrotaline and ultrasonographic study of right ventricular remodeling

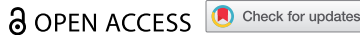
Jing Dong, Xiao-Min Jiang, Du-Jiang Xie, Jie Luo, Hong Ran, Lin Li, Miao Li, Pei Jiang, Ping-Yang Zhang & Ling Zhou

To cite this article: Jing Dong, Xiao-Min Jiang, Du-Jiang Xie, Jie Luo, Hong Ran, Lin Li, Miao Li, Pei Jiang, Ping-Yang Zhang & Ling Zhou (2023) Establishment of a canine model of pulmonary arterial hypertension induced by dehydromonocrotaline and ultrasonographic study of right ventricular remodeling, Clinical and Experimental Hypertension, 45:1, 2190503, DOI: 10.1080/10641963.2023.2190503

To link to this article: https://doi.org/10.1080/10641963.2023.2190503

9	© 2023 The Author(s). Published with license by Taylor & Francis Group, LLC.	Published online: 16 Mar 2023.
	Submit your article to this journal 🗗	Article views: 222
Q ^L	View related articles 🗹	View Crossmark data 🗹







Establishment of a canine model of pulmonary arterial hypertension induced by dehydromonocrotaline and ultrasonographic study of right ventricular remodeling

Jing Dong^a†, Xiao-Min Jiang^b†, Du-Jiang Xie^b, Jie Luo^b, Hong Ran^a, Lin Li^a, Miao Li^a, Pei Jiang^a, Ping-Yang Zhang^a, and Ling Zhoub

^aDepartment of Cardiovascular Ultrasound, Nanjing First Hospital, Nanjing Medical University, Nanjing, Jiangsu Province, China; ^bDepartment of Cardiology, Nanjing First Hospital, Nanjing Medical University, Nanjing, Jiangsu Province, China

ABSTRACT

Objective: Pulmonary arterial hypertension (PAH) means high blood pressure in the lungs. We aimed to observe the right ventricular size, wall thickness and characteristic functional changes and their associations with PAH in an established model of beagle dogs, and to explore convenient, reliable and sensitive ultrasound indicators for assessing right ventricular remodeling.

Methods: Twenty healthy beagle dogs (8-10 kg) were randomly divided into control group (N-dimethylformamide, n = 10) and dehydromonocrotaline (DHMCT) group (DHMCT, n = 10). N-dimethylformamide or DHMCT was injected through a catheter into the right atrium, and then right heart catheterization, routine echocardiography and two-dimensional speckle tracking imaging (2D-STI) were performed before modeling (0 weeks) and 8, 14 weeks after modeling. Hemodynamic parameters and right ventricular function-related ultrasound data were acquired. At the end of the experiment, the animals were killed and the lung tissues were taken for HE staining. Left and right ventricular walls were separated and weighed respectively, and right ventricular hypertrophy index (RVHI) was measured. The associations of the routine ultrasound data and 2D-STI data at each time point with hemodynamic parameters and RVHI were analyzed.

Results: At 0, 8 and 14 weeks, gradual decreases in the right ventricular global longitudinal strain (RVLS) were found in DHMCT group. RVH occurred in DHMCT group, and DHMCT group had a significantly higher RVHI than that of control group ($49.83 \pm 4.83\%$ vs. $39.80 \pm 1.40\%$, P < .001) and larger pulmonary artery media thickness. RVLS had significant positive correlations with RVSP (r = 0.74, P < .001), mRVP (r = 0.74), mRVP 0.72, P < .001), PASP (r = 0.75, P < .001), mPAP (r = 0.72, P < .001) and PVR (r = 0.68, P < .001). There was a significant positive correlation between RVLS and RVHI (r = 0.74, P < .001).

Conclusion: The right ventricular function in PAH can be effectively assessed by echocardiography, and RVLS measured by 2D-STI sensitively reflects right ventricular remodeling following PAH.

ARTICLE HISTORY

Received 15 November 2022 Revised 28 February 2023 Accepted 9 March 2023

KEYWORDS

Dehydromonocrotaline: pulmonary arterial hypertension; right ventricular remodeling; echocardiography; twodimensional speckle tracking

Introduction

At present, pulmonary arterial hypertension (PAH) has been widely studied. Many methods are available to establish animal models of PAH, mainly including hypoxia, monocrotaline (MCT), shunt surgery, single lobectomy and neointimal method, and they can be used alone or combined. However, no model can completely replicate the pathological changes in human PAH so far (1,2). Mice, rats, dogs, sheep, pigs and cattle are commonly used laboratory animals for PAH models. Percutaneous catheter intervention was performed in this study, which was suitable only for large mammals. With similar anatomy and physiology of the heart to humans, beagle dogs are docile and can be fed easily. Therefore, healthy adult beagle dogs were selected as laboratory animals in this study. MCT is a pyrrolizidine alkaloid, and it has been proven to be able to cause PAH in rats 50 years ago (3). MCT is biologically inactive and is metabolized by hepatic cytochrome P450 monooxygenases into a bifunctional cross-linked complex, dehydromonocrotaline (DHMCT), which enters the lung through blood circulation, causing irreversible damage to the pulmonary artery (4,5). MCT-induced PAH has a similar pathogenesis to connective tissue-related PAH, and MCTinduced modeling is characterized by simple operation, good repeatability, easy availability of reagents, low overall costs and small time consumption, so it has been the most commonlyused method for animal modeling of PAH. Due to the lack of P450 monooxygenases in the canine liver, however, DHMCT needs to be synthesized in vitro and injected prior to PAH modeling. Echocardiography is convenient, efficient, simple, highly repeatable and free of side effects, so it can serve as the preferred method for dynamic observation of animal models and evaluation of modeling effects.

Nevertheless, the currently available routine echocardiographic indicators have limitations and are restricted by external conditions. Therefore, we need to explore more sensitive and convenient ultrasonic indicators to reflect the right

CONTACT Ping-Yang Zhang 🔯 zhpy28@hotmail.com 🗊 Department of Cardiovascular Ultrasound, Nanjing First Hospital, Nanjing Medical University, Nanjing, Jiangsu Province 210006, China; Ling Zhou 🔯 zhoulingnfh@dh-edu.cn 🗈 Department of Cardiology, Nanjing, Jiangsu Province 210006, China

ventricular function. This study was thus performed to observe the process of DHMCT-induced canine PAH modeling by routine echocardiography and two-dimensional speckle tracking imaging (2D-STI), to determine whether the animal model was stable and reliable by these two techniques combined with echocardiographic indicators reflecting right ventricular remodeling, and to search convenient, reliable and sensitive ultrasound indicators for assessing right ventricular remodeling in the case of PAH.

Materials and Methods

Grouping

The study has received ethical approval by the animal ethical committee of Nanjing First Hospital, Nanjing Medical University (approval No. NJMEDHOS 76895211) and followed the National Research Council for animal research. A total of 20 beagle dogs were randomly divided into control group (3 mg/kg N-dimethylformamide injected into the right atrium, n = 10) and DHMCT group (3 mg/kg DHMCT injected into the right atrium, n = 10). At 14 weeks, all animals were subjected to right heart catheterization (RHC) and transthoracic echocardiography (TTE) and sacrificed. Then heart and lung tissues were isolated and stored at -80°C for further pathological and molecular biological analysis. The flow chart for experiments is shown in Figure 1.

Hemodynamic measurement

After intravenous anesthesia with 30 mg/kg pentobarbital sodium, the animal was fixed on an operating table in a supine position in the catheterization room and connected with an ECG monitoring device and a percutaneous oxygen saturation detector, and venous access was opened for tracheal intubation and connected to an animal ventilator, followed by mechanical

ventilation with a tidal volume of 150 mL. Pentobarbital sodium was intravenously infused at 1 mg/min for maintenance of anesthesia. The right femoral vein was punctured with a 7F arterial sheath, and a 5F Swan-Ganz catheter connected with a pressure transducer was inserted to successively measure the right atrial pressure (RAP), right ventricular pressure (RVP), pulmonary arterial pressure (PAP) and pulmonary capillary wedge pressure (PCWP). Cardiac output (CO) was measured by thermodilution. All parameters were measured 3 times and the average was taken. Pulmonary vascular resistance (PVR)= (mPAP-PCWP)/CO. The above hemodynamic parameters were measured repeatedly at 0, 8, and 14 weeks for each animal in both groups.

Routine echocardiography and 2D-STI

Echocardiography was performed using GE Vivid7 ultrasound diagnostic system (M4S transducer, frequency: 1.4-4.3 MHz). Under general anesthesia, the beagle dogs were placed in a supine position and received ECG monitoring, and the following ultrasound parameters of right ventricular function were assessed in a conventional view: right ventricular diameter (RV), right ventricular wall thickness (RVW), interventricular septal thickness (IVS), tricuspid annular plane systolic excursion (TAPSE), Tei index and tricuspid annular peak systolic velocity (S'). The right ventricular end-diastolic area (RVEDA) and right ventricular end-systolic area (RVESA) were measured in the apical four-chamber view dominated by the right ventricle, and the right ventricular fractional area change (RVFAC) was calculated: RVFAC=(RVEDA-RVESA)/RVEDA × 100%. Apical four-chamber echocardiography 2D dynamic images were acquired for at least 3 cardiac cycles, and imported into the EchoPAC workstation for offline analysis. The endocardial surface of right ventricle was delineated by 2D strain analysis software when the endocardial surface on the 2D image was most clearly shown (end-systole). The region of interest could be

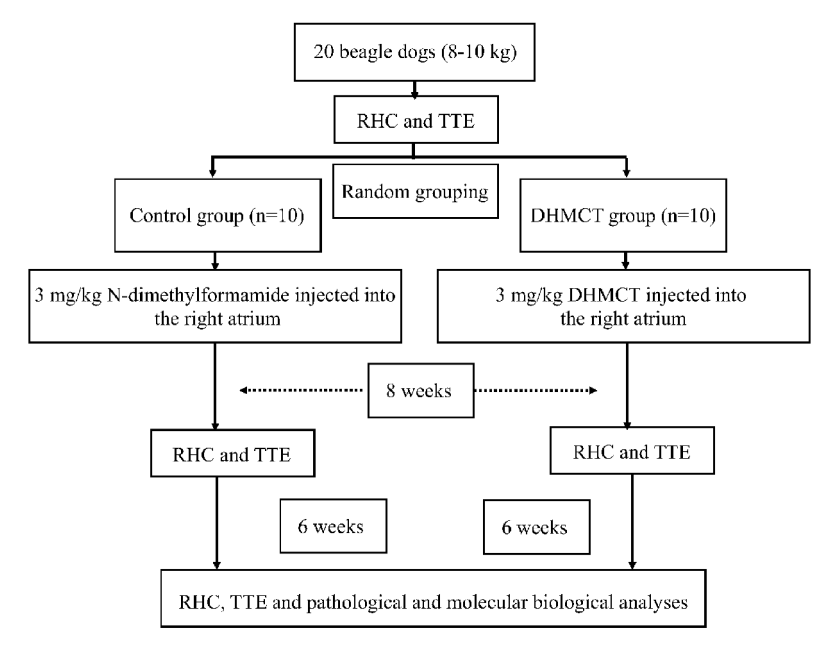


Figure 1. Flow chart for experiments.

automatically generated by the software, and its width was manually adjusted to coincide with RVW. Following the program run, the motion trajectory of myocardial speckles in the region of interest was automatically tracked frame by frame. The right ventricular free wall and interventricular septum were divided into epicardial layer, middle lay and endocardial layer, and each layer was further divided into apical segment, middle segment and basal segment. The myocardial time-longitudinal strain and strain rate curves of myocardium in each segment of each layer meeting the conditions for myocardial speckle tracking were automatically generated by the software, and the longitudinal peak systolic strain (S), peak systolic strain rate (SRs), early diastolic strain rate (SRe) and late diastolic strain rate (SRa) in each segment of each layer were measured. The above echocardiographic and 2D-STI parameters were measured repeatedly at 0, 8, and 14 weeks for each animal in both groups.

Sample treatment

After the experimental period, the animals were sacrificed by an overdose of pentobarbital sodium, and the carotid artery was cut open to allow exsanguination. The thoracic cavity was quickly cut open, and the heart and lung tissues were isolated and washed with normal saline to remove residual blood. The pericardium was opened to determine the position of the right ventricle, based on which the position of the pulmonary artery was identified. The pulmonary artery and its main left and right branches were quickly isolated and harvested. The lung tissues (about $10 \times 10 \times 10$ mm) near the hilum of lung were harvested, washed with normal saline to remove residual blood, and fixed with neutral formaldehyde for 72 h.

Measurement of RVHI

After the animals were sacrificed and the heart and lung tissues were isolated, the heart was harvested, and the residual blood was washed away. The left and right atrial tissues and great vessels were removed along the atrioventricular groove, the right ventricular free wall tissues were cut off along the right edge of the interventricular septum, and the redundant fat and valve tissues were removed. The left ventricle and interventricular septum were cut open, and the blood in the left ventricle was cleared. The tissue weights of right ventricular free wall (RV) and left ventricular free wall + interventricular septum (LV+S) were measured, and RVHI was calculated finally: RVHI=RV/(LV+S).

Hematoxylin-eosin (HE) staining

The embedded paraffin tissue was cut into 3 µm-thick sections, and HE staining was performed according to routine steps. The inner diameter and media thickness of pulmonary arterioles were observed.

Statistical analysis

SPSS 22.0 software was used for statistical analysis. Measurement data were expressed as mean ± standard

deviation ($\bar{x} \pm s$). Repeated measures analysis of variance was performed for intragroup comparison, and the paired-samples *t*-test was conducted for intergroup comparison. *P* <0.001 was considered statistically significant.

Results

Mortality rate

Four animals died in DHMCT group, with a mortality rate of 40%, while no animals died in control group.

Hemodynamic parameters detected by RHC

There were no statistically significant differences in hemodynamic parameters between the two groups before medication, and the hemodynamic parameters in control group remained stable throughout the experiment.

At 8 weeks after modeling, the right ventricular systolic pressure (RVSP), mean RVP (mRVP), pulmonary arterial systolic pressure (PASP), mPAP and PVR all significantly rose in DHMCT group, and they were all significantly higher than those in control group.

At 14 weeks after modeling, the RVSP, mRVP, mPAP, PASP and PVR further rose in DHMCT group, and they were also significantly higher than those in control group (Table 1), suggesting that the canine PAH model was successfully established with DHMCT.

Routine echocardiographic results

Routine echocardiographic parameters had no statistically significant differences between the two groups before medication, and the routine echocardiographic parameters in control group remained stable throughout the experiment.

At 8 weeks after modeling, RVW, IVS and Tei index in DHMCT group all increased compared with those at 0 weeks and in control group. TAPSE in DHMCT group was not significantly different from that at 0 weeks and in control group.

At 14 weeks after modeling, both RVW and IVS further increased in DHMCT group, the Tei index had no significant change compared with that at 0 and 8 weeks and in control group, and TAPSE significantly declined compared with that at 0 weeks and in control group.

The changes in RV, RVFAC and S' had no statistically significant differences throughout the experiment (Table 2 and Figure 2).

2D-STI results

At 0, 8 and 14 weeks, significant gradual decreases in the right ventricular global longitudinal strain (RVLS) could be seen in DHMCT group. Both GSRs and GSRa in DHMCT group were lower than those in control group at 14 weeks, while GSRe had no great changes (Table 3 and Figure 3).

Table 1. Hemodynamic data of control and DHMCT groups.

Parameter	Time	Control (<i>n</i> = 10)	DHMCT $(n = 6)$	P value
mRAP (mmHg)	0 week	1.60 ± 0.84	1.17 ± 0.75	0.319
	8th week	1.80 ± 0.92	2.50 ± 1.05	0.183
	14th week	2.30 ± 0.95	2.50 ± 1.64	0.760
RVSP (mmHg)	0 week	31.61 ± 3.16	34.33 ± 6.25	0.356
	8th week	33.07 ± 2.88	49.67 ± 8.73	0.005
	14th week	36.14 ± 3.59	58.70 ± 5.33	< 0.001
mRVP (mmHg)	0 week	10.24 ± 1.65	9.83 ± 3.66	0.762
	8th week	10.97 ± 1.57	15.00 ± 3.10	0.004
	14th week	12.35 ± 1.41	18.71 ± 2.13	< 0.001
PASP (mmHg)	0 week	28.07 ± 2.29	27.17 ± 2.86	0.496
	8th week	29.99 ± 1.87	44.83 ± 6.46	0.002
	14th week	31.77 ± 2.64	54.58 ± 7.33	< 0.001
mPAP (mmHg)	0 week	15.40 ± 2.14	13.00 ± 2.61	0.065
	8th week	16.81 ± 1.38	29.50 ± 5.05	0.001
	14th week	17.49 ± 2.34	35.31 ± 6.14	< 0.001
PVR (Woods unit)	0 week	3.09 ± 0.44	2.50 ± 0.44	0.021
	8th week	3.02 ± 0.40	6.59 ± 1.50	0.002
	14th week	2.61 ± 0.49	7.82 ± 3.19	0.010
CO (I/min)	0 week	3.36 ± 0.31	3.50 ± 0.91	0.733
	8th week	3.83 ± 0.76	3.53 ± 0.57	0.481
	14th week	4.28 ± 1.04	4.21 ± 1.33	0.898

mRAP: Mean right atrial pressure, RVSP: right ventricular systolic pressure, mRVP: mean right ventricular pressure, PASP: pulmonary arterial systolic pressure, mPAP: mean pulmonary arterial pressure, PVR: pulmonary vascular resistance, CO: cardiac output.

Table 2. Routine echocardiographic data of control and DHMCT groups.

Parameter	Time	Control $(n = 10)$	DHMCT $(n = 6)$	P value
RV (mm)	0 week	11.75 ± 1.28	11.16 ± 0.87	0.341
	8th week	12.15 ± 1.37	12.50 ± 0.65	0.495
	14th week	12.47 ± 1.02	12.83 ± 0.67	0.456
RVW (mm)	0 week	3.15 ± 0.20	3.14 ± 0.19	0.927
	8th week	3.13 ± 0.17	4.92 ± 0.50	< 0.001
	14th week	3.17 ± 0.17	5.35 ± 0.46	< 0.001
IVS (mm)	0 week	6.09 ± 0.38	6.22 ± 0.39	0.510
	8th week	6.44 ± 0.52	7.15 ± 0.55	0.022
	14th week	6.49 ± 0.67	7.63 ± 0.32	< 0.001
RVFAC (%)	0 week	53.91 ± 4.64	55.27 ± 6.95	0.645
	8th week	53.60 ± 4.33	53.95 ± 7.52	0.920
	14th week	53.79 ± 4.42	52.83 ± 7.01	0.741
TAPSE (mm)	0 week	8.88 ± 0.73	9.07 ± 0.75	0.619
	8th week	8.84 ± 0.65	7.96 ± 1.10	0.060
	14th week	8.65 ± 0.83	6.49 ± 0.64	< 0.001
TDI S' (cm/sec)	0 week	10.14 ± 1.33	11.68 ± 1.35	0.042
(*,	8th week	10.66 ± 1.66	9.35 ± 1.17	0.113
	14th week	11.69 ± 1.13	10.28 ± 2.33	0.123
Tei (RV)	0 week	0.37 ± 0.07	0.39 ± 0.02	0.404
	8th week	0.34 ± 0.05	0.54 ± 0.10	< 0.001
	14th week	0.35 ± 0.07	0.48 ± 0.14	0.064

RV: Right ventricular diameter, RVW: right ventricular wall thickness, IVS: interventricular septal thickness, RVFAC: right ventricular fractional area change, TAPSE: tricuspid annular plane systolic excursion, TDI S:' tissue Doppler imaging tricuspid annular peak systolic velocity.

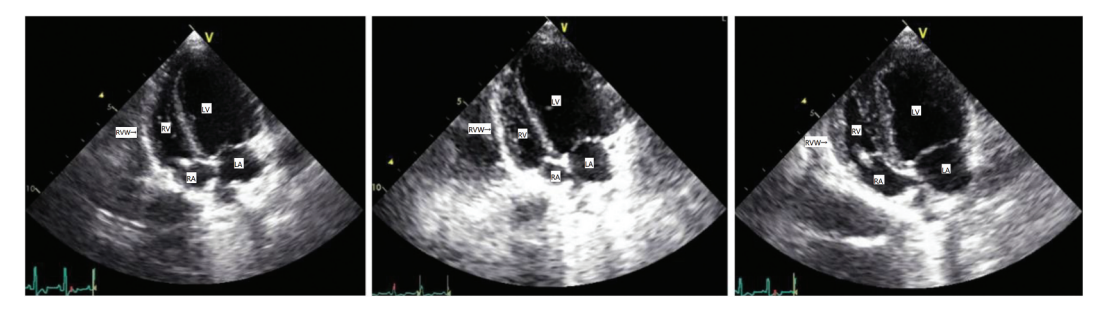


Figure 2. Apical four-chamber echocardiography images at 0, 8 and 14 weeks in DHMCT group.

Table 3. 2D-STI data of control and DHMCT groups.

Parameter	Time	Control (<i>n</i> = 10)	DHMCT $(n = 6)$	P value
RVLS endo (%)	0 week	-23.26 ± 2.66	-23.58 ± 2.36	0.810
	8th week	-24.13 ± 3.00	-19.03 ± 2.11	0.003
	14th week	-23.18 ± 2.90	-14.68 ± 3.40	< 0.001
RVLS mid (%)	0 week	-19.35 ± 1.73	-19.50 ± 1.65	0.867
	8th week	-19.69 ± 2.02	-14.88 ± 2.02	< 0.001
	14th week	-19.39 ± 1.86	-10.65 ± 2.41	< 0.001
RVLS epi (%)	0 week	-15.63 ± 1.36	-16.10 ± 1.39	0.517
	8th week	-15.71 ± 1.40	-11.58 ± 2.29	< 0.001
	14th week	-16.06 ± 1.43	-7.57 ± 2.28	< 0.001
GSR s (1/sec)	0 week	-2.19 ± 0.36	-2.13 ± 0.40	0.774
	8th week	-2.04 ± 0.42	-1.57 ± 0.42	0.048
	14th week	-2.04 ± 0.28	-1.50 ± 0.21	0.001
GSR e (1/sec)	0 week	1.43 ± 0.60	1.00 ± 0.55	0.176
, ,	8th week	1.02 ± 0.43	0.75 ± 0.19	0.106
	14th week	0.96 ± 0.35	0.57 ± 0.43	0.067
GSR a (1/sec)	0 week	2.44 ± 0.71	2.47 ± 1.03	0.952
	8th week	2.37 ± 0.40	1.82 ± 0.67	0.056
	14th week	2.69 ± 0.74	1.48 ± 0.40	0.002

RVLS-endo: right ventricular endocardial longitudinal strain, RVLS-mid: right ventricular myocardial longitudinal strain, RVLS-epi: right ventricular epicardial longitudinal strain, GSRs: global peak systolic strain rate, GSRe: global peak early diastolic strain rate, GSRa: global peak late diastolic strain rate.

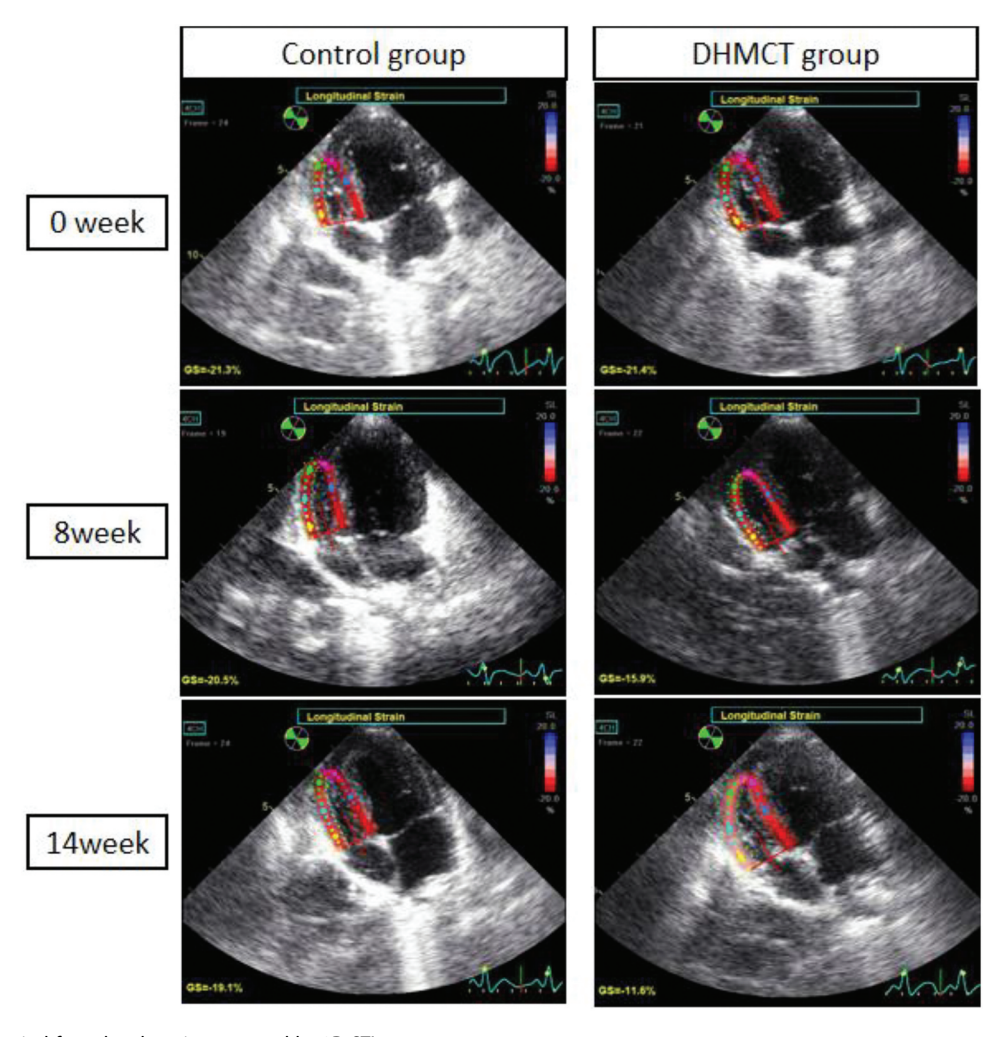


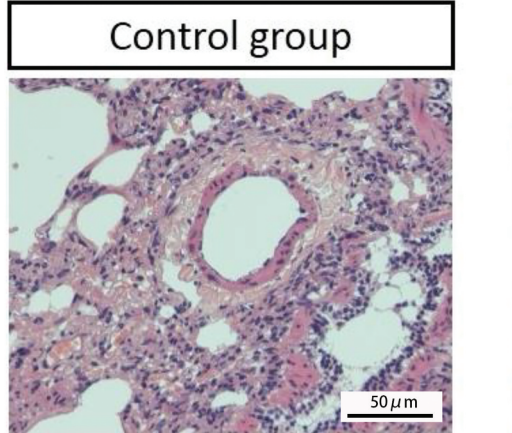
Figure 3. RVLS in the apical four-chamber view assessed by 2D-STI.

Change in RVHI

RVH occurred in DHMCT group, and DHMCT group had a significantly higher RVHI than control group [(49.83 \pm 4.83)% *vs.* (39.80 \pm 1.40)%, $P \le .001$)].

Results of HE staining of lung tissues

DHMCT group had significantly larger pulmonary artery media thickness and significantly smaller lumen than control group (optical microscope, ×100) (Figure 4).



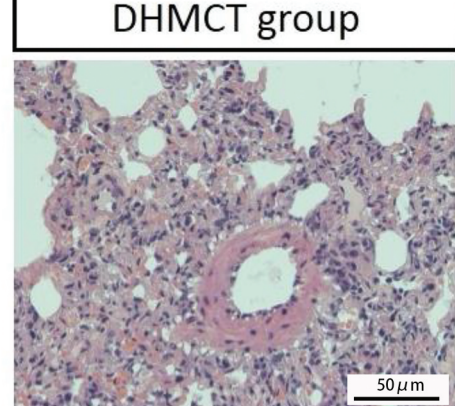


Figure 4. Results of HE staining of lung tissues.

Associations of RVLS with hemodynamic parameters and **RVHI**

RVLS was highly correlated with hemodynamic parameters, i.e., it had significant positive correlations with RVSP (r = 0.74, P < .001), mRVP (r = 0.72, P < .001), PASP (r = 0.75, P < .001), mPAP (r = 0.72, P < .001) and PVR (r = 0.68, P < .001)(Figure 5). Besides, there was a high positive correlation between RVLS and RVHI (r = 0.74, P < .001) (Figure 6).

Discussion

The pathogenesis of PAH remains to be studied, but pulmonary artery remodeling including muscular pulmonary artery intimal thickening, precapillary arteriolar muscularization and pulmonary vascular obstruction has been verified to be the common characteristic pathological change of PAH (6). Animal models of diseases are helpful for studying the pathogenesis, pathological changes and new treatment methods of

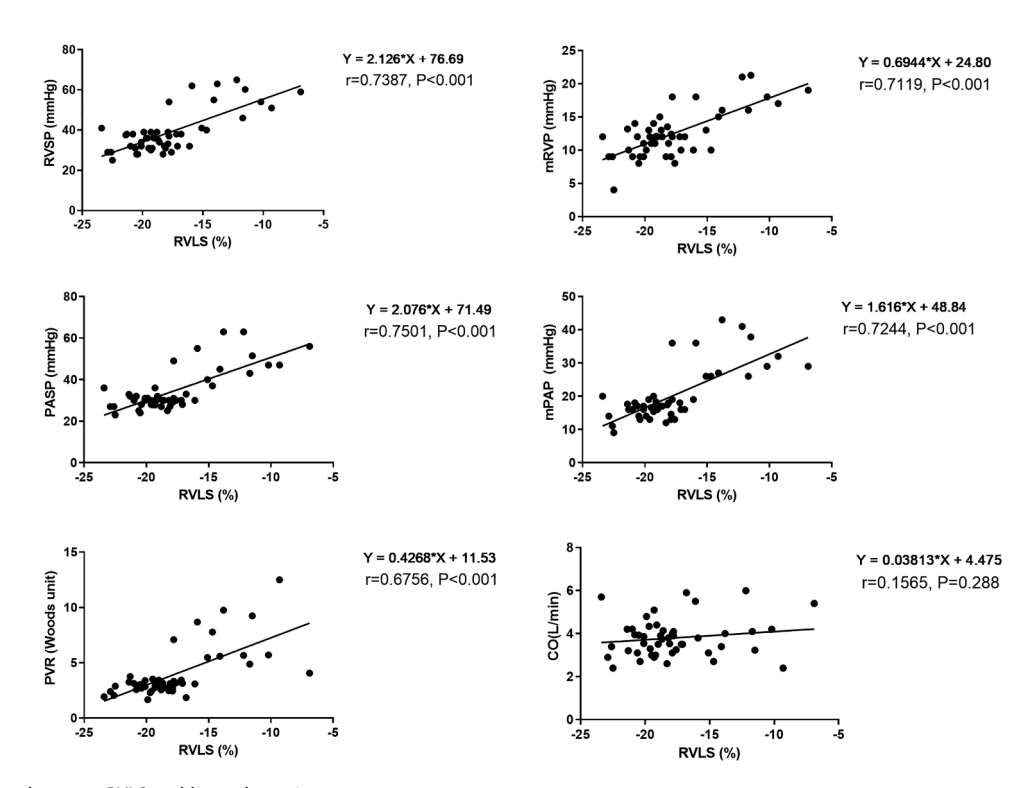


Figure 5. Associations between RVLS and hemodynamic parameters.

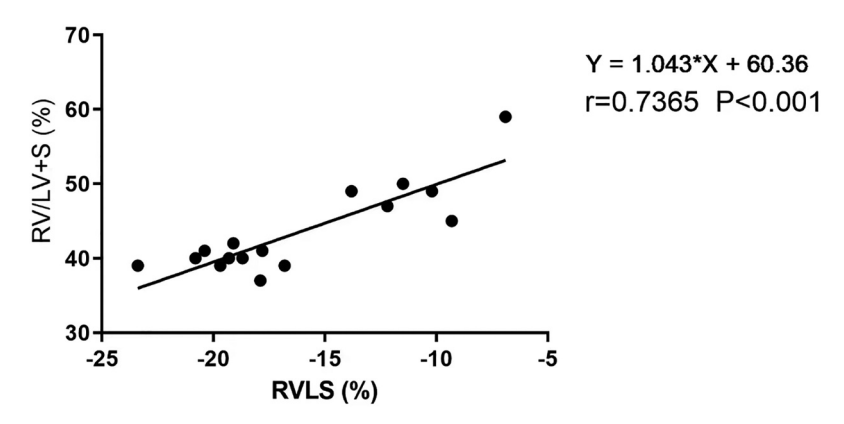


Figure 6. Associations between RVLS and RVHI.

corresponding diseases. MCT-induced modeling characterized by simple operation, good repeatability and small time consumption has been widely applied in PAH research. MCT is biologically inactive and metabolized by hepatic cytochrome P450 monooxygenases into active DHMCT, which enters lung tissues through blood circulation. The mechanism by which DHMCT induces PAH is not entirely clear, probably involving pulmonary artery endothelial cell injury and vascular adventitia injury. At the early stage of MCT administration, a large number of inflammatory cells accumulate in the pulmonary artery adventitia, and then vascular remodeling gradually emerges, suggesting the important role of adventitia during pulmonary artery remodeling (7,8). Unlike humans and rats, dogs lack CYP3A4 in the liver, so active DHMCT, which cannot be converted from MCT, needs to be synthesized in vitro. However, DHMCT is extremely unstable and easily decomposed at normal temperature and in aqueous solution (e.g. plasma), with a half-life<14 s, so it needs to be prepared immediately before use (9,10). DHMCT induces irreversible damage to the canine pulmonary artery. Previous studies mostly focused on DHMCT at about 8 weeks after injection, whereas there are few reports over a longer period of time.

In this study, it was confirmed through a 14-week observation period that after 3 mg/kg DHMCT was injected into the right atrium in beagle dogs, RVSP, PASP, mPAP and PVR all showed a trend of gradual increase and were significantly higher than those in control group at 8 and 14 weeks, right ventricular remodeling also occurred, and RVW gradually rose. It can be seen that injection of 3 mg/kg DHMCT into the right atrium could be used to successfully establish the stable canine PAH model, and the hemodynamic and pathological changes in this model could last until the 14th week, thereby ensuring the reliability and stability of this model. However, the mortality rate of animals increased with time. Specifically, the mortality rate of DHMCT-induced PAH dogs was about 20% previously but up to 40% in this study. Laboratory animal death could be still seen after 8 weeks, which was closely related to the worsened right heart failure and long duration of PAH.

Among examinations for PAH, RHC remains the gold standard for the detection and diagnosis of PAH, but it, as an invasive examination, cannot be used routinely. Cardiac magnetic resonance imaging (CMRI) has always been the gold standard for noninvasive assessment of right ventricular function, but it is difficult to popularize in primary hospitals due to its high costs, large time consumption and complicated operation. Echocardiography characterized by convenience, accuracy, good repeatability and high correlation with heart catheterization results has become the most important noninvasive examination for PAH screening. The important role of echocardiography in the assessment of right ventricular function has been demonstrated in many previous studies. Miller et al. found that TAPSE was an indicator for determining the right ventricular function, and TAPSE<15 mm indicated an abnormal right ventricular systolic function (11). RVFAC<35% corresponds to a decline in right ventricular ejection fraction (RVEF). RVFAC has a good correlation with RVEF measured by MRI and changes with the progression of PAH (12). Proposed by Tei (a Japanese scholar) in 1995, myocardial performance index (MPI) is an indicator for comprehensively assessing the cardiac systolic and diastolic functions, which is also known as Tei index (13,14). As recommended by the American Society Echocardiography guidelines in 2010 (15), S' <10 cm/s can be used as an effective indicator for abnormal right ventricular function. In recent years, 2D strain imaging technique has been increasingly studied, which is a new ultrasonic quantitative analysis technique based on judging the motion velocity gradient between two points in the myocardium. Myocardial strain and strain rate reflect the deformability of myocardium, the myocardial motion state more intuitively and accurately, and also the local and overall myocardial systolic function (16,17). TDI and STI are used to assess the myocardial strain and strain rate currently. In recent years, 2D-STI has been rapidly developed, which identifies numerous acoustic speckles in the myocardium in 2D grayscale images and automatically tracks their motion during myocardial systolic motion, thereby acquiring the motion characteristics of myocardial tissues, and then it obtains the myocardial strain and strain rate by calculating the distance change between two adjacent speckles. The research reported that there was a significantly lower RVLS in patients with severe PH than that in patients with mild PH, and RVLS was associated with RVEF measured by CMRI (18,19). However,

few studies have been conducted on the correlation of RVLS with right ventricular remodeling. In this study, the whole modeling process was observed dynamically by echocardiography, the routine echocardiographic data of right ventricular function were recorded at different time points in both groups, and the 2D strain and strain rate were measured by 2D-STI. Moreover, the associations of the routine ultrasound data and 2D-STI data with hemodynamic parameters and RVHI were analyzed. The results showed that RVW and IVS gradually increased, while Tei index and TAPSE had changes in DHMCT group but showed no statistically significant difference between the adjacent two time points, and no obvious changes were observed in RV, RVFAC and S' throughout the experiment. The possible reason is that the observation period was short and the early right ventricular remodeling cannot be estimated by these data. Besides, RVLS measured by 2D-STI showed a significant trend of gradual decrease at 0, 8 and 14 weeks, and it had a statistically significant difference between the adjacent two time points. According to routine echocardiographic data combined with 2D-STI data, the right ventricular function was damaged and right ventricular remodeling occurred after 3 mg/kg DHMCT was injected into the right atrium of beagle dogs, further proving that DHMCT can successfully induce stable canine PAH models. In addition, the routine echocardiographic data and 2D-STI data at different time points were statistically analyzed in both groups. It was found that RVLS could reflect right ventricular remodeling more sensitively than other data, and it had a significant positive correlation with hemodynamic data measured by RHC and a moderate positive correlation with RVHI. It can be inferred that RVLS measured by 2D-STI is sensitive in reflecting right ventricular remodeling following PAH, and it can be applied to clinical and experimental research as an important indicator for assessing right ventricular remodeling in PAH.

Conclusion

In conclusion, the canine PAH model can be successfully established by injection of DHMCT (3 mg/kg) into the right atrium. The right ventricular function in PAH can be dynamically assessed by echocardiography, and RVLS measured by 2D-STI can sensitively reflect right ventricular remodeling following PAH.

Statement of Ethical Approval

The study has received ethical approval by the animal ethical committee of Nanjing First Hospital, Nanjing Medical University (approval No. NJMEDHOS 76895 211) and followed the National Research Council for animal research.

Disclosure statement

No potential conflict of interest was reported by the author(s).

Funding

The author(s) reported there is no funding associated with the work featured in this article.

References

- 1. Holmes D, Corr M, Thomas G, Harbinson M, Campbell M, Spiers P, Bell D. Protective effects of intermedin/adrenomedullin-2 in a cellular model of human pulmonary arterial hypertension. Peptides. 2020;126:170267. doi:10.1016/j.peptides. 2020.170267.
- 2. Agarwal S, Harter ZJ, Krishnamachary B, Chen L, Nguyen T, Voelkel NF, Nk D. Sugen-morphine model of pulmonary arterial hypertension. Pulm Circ. 2020; 10(1):2045894019898376. doi:10. 1177/2045894019898376.
- 3. Suslonova OV, Smirnova SL, Roshchevskaya IM. Cardiac body surface potentials in rats with experimental pulmonary hypertension during ventricular depolarization. Bull Exp Biol Med. 2016; 162(1):7-10. doi:10.1007/s10517-016-3531-y.
- 4. Wang XM, Shi K, Li JJ, Chen TT, Guo YH, Liu YL, Yang YF, Yang S. Effects of angiotensin II intervention on MMP-2, MMP-9, TIMP-1, and collagen expression in rats with pulmonary hypertension. Genet Mol Res. 2015; 14(1):1707-17. doi:10.4238/ 2015.March.6.17.
- 5. de Lima-Seolin BG, Hennemann MM, Fernandes RO, Colombo R, Bonetto JHP, Teixeira RB, Khaper N, Godoy AEG, Litvin IE, Sander da Rosa Araujo A, et al. Bucindolol attenuates the vascular remodeling of pulmonary arteries by modulating the expression of the endothelin-1 a receptor in rats with pulmonary arterial hypertension. Biomed Pharmacother. 2018;99:704-14. doi:10. 1016/j.biopha.2018.01.127.
- 6. Rafikova O, Al Ghouleh I, Rafikov R. Focus on early events: pathogenesis of pulmonary arterial hypertension development. Antioxid Redox Signal. 2019; 31(13):933-53. doi:10.1089/ars.2018.7673.
- 7. Zimmer A, Teixeira RB, Constantin RL, Campos-Carraro C, Aparicio Cordero EA, Ortiz VD, Donatti L, Gonzalez E, Bahr AC, Visioli F, et al. The progression of pulmonary arterial hypertension induced by monocrotaline is characterized by lung nitrosative and oxidative stress, and impaired pulmonary artery reactivity. Eur J Pharmacol. 2021;891:173699. doi:10.1016/j.ejphar. 2020.173699.
- 8. Tian L, Wu D, Dasgupta A, Chen KH, Mewburn J, Potus F, Lima PDA, Hong Z, Zhao YY, Hindmarch CCT, et al. Epigenetic metabolic reprogramming of right ventricular fibroblasts in pulmonary arterial hypertension: a pyruvate dehydrogenase kinase-dependent shift in mitochondrial metabolism promotes right ventricular fibrosis. Circ Res. 2020; 126(12):1723-45. doi:10.1161/CIRCRESAHA.120.316443.
- 9. Yang L, Zhang L, Chen S, Li M, Long Y, Li W, Jin Q, Guan L, Zhou D, Ge J. Efficacy of interatrial shunt devices: an opening window to acute pulmonary hypertensive crisis and chronic pulmonary arterial hypertension. J Thromb Thrombolysis. 2022; 54(1):123-31. doi:10.1007/s11239-022-02635-3.
- 10. Constantine A, Dimopoulos K. Pulmonary artery denervation for pulmonary arterial hypertension. Trends Cardiovasc Med. 2021; 31(4):252-60. doi:10.1016/j.tcm.2020.04.005.
- 11. Miller D, Farah MG, Liner A, Fox K, Schluchter M, Bd H. The relation between quantitative right ventricular ejection fraction and indices of tricuspid annular motion and myocardial performance. J Am Soc Echocardiogr. 2004; 17(5):443-47. doi:10. 1016/j.echo.2004.01.010.
- 12. Kasprzak JD, Huttin O, Wierzbowska-Drabik K, Selton-Suty C. Imaging the right heart-pulmonary circulation unit: the role of ultrasound. Heart Fail Clin. 2018; 14(3):361-76. doi:10.1016/j.hfc.
- 13. Chuwa T, Rodeheffer RJ. New index of combined systolic and diastolic myocardial performance: a simple and reproducible measure of cardiac function—a study in normals and dilated cardiomyopathy. J Cardiol. 1995;26(35):357-66. PMID: 8558414.



- 14. Friesen RM, Schäfer M, Jone PN, et al. Myocardial Perfusion Reserve Index in Children with Kawasaki Disease. J Magn Reson Imaging. 2018;48(1):132–39. doi:10.1002/jmri.25922.
- 15. Rudski LG, Lai WW, Afilalo J, Hua L, Handschumacher MD, Chandrasekaran K, Solomon SD, Louie EK, Nb S. Guidelines for the echocardiographic assessment of the right heart in adults: a report from the American Society of Echocardiography: endorsed by the European association of echocardiography, a registered branch of the European society of cardiology, and the Canadian society of echocardiography. J Am Soc Echocardiogr. 2010; 23 (7):685–713. doi:10.1016/j.echo.2010.05.010.
- Lin ACW, Seale H, Hamilton-Craig C, Morris NR, Strugnell W. Quantification of biventricular strain and assessment of ventriculo-ventricular interaction in pulmonary arterial hypertension using exercise cardiac magnetic resonance imaging and myocardial feature tracking. J Magn Reson Imaging. 2019; 49(5):1427–36. doi:10. 1002/jmri.26517.
- 17. Mansell DS, Bruno VD, Sammut E, Chiribiri A, Johnson T, Khaliulin I, Lopez DB, Gill HS, Fraser KH, Murphy M, et al. Acute regional changes in myocardial strain may predict ventricular remodelling after myocardial infarction in a large animal model. Sci Rep. 2021; 11(1):18322. doi:10.1038/s41598-021-97834-y.
- 18. Li Y, Xie M, Wang X, Lu Q, Fu M. Right ventricular regional and global systolic function is diminished in patients with pulmonary arterial hypertension: a 2-dimensional ultrasound speckle tracking echocardiography study. Int J Cardiovasc Imaging. 2013; 29(3):545–51. doi:10.1007/s10554-012-0114-5.
- 19. Li AL, Zhai ZG, Zhai YN, Xie WM, Wan J, Tao XC. The value of speckle-tracking echocardiography in identifying right heart dysfunction in patients with chronic thromboembolic pulmonary hypertension. Int J Cardiovasc Imaging. 2018; 34(12):1895–904. doi:10.1007/s10554-018-1423-0.